Acid–base properties and DNA-binding of water soluble N-confused porphyrins with cationic side-arms†

Yoshiya Ikawa,[a,b] Shoji Moriyama,[a] Hiroyuki Harada[a] and Hiroyuki Furuta*[a]

Received 16th June 2008, Accepted 29th July 2008
First published as an Advance Article on the web 16th September 2008
DOI: 10.1039/b810171j

Water soluble N-confused porphyrins, 5,10,15,20-tetrakis(α-pyridinio-*p*-tolyl)-2-aza-21-carbaporphyrin (**pPyNCP**) and its *N*-methyl derivative, 2-*N*-methyl-5,10,15,20-tetrakis(α-pyridinio-*p*-tolyl)-2-aza-21-carbaporphyrin (**NMe-pPyNCP**), have been synthesized by introducing cationic side-arms at the *meso*-positions of N-confused porphyrin. Their acid–base properties (pK_{1-4}) and DNA-binding ability in aqueous solutions were elucidated in comparison with the corresponding porphyrin derivative. Photophysical behaviors of **pPyNCP** were largely influenced by buffer compositions and DNA structures, whereas **NMe-pPyNCP** is considerably robust against these factors. In addition, significant enhancement of the fluorescence was observed with **NMe-pPyNCP** by the addition of DNA. The unique properties of **pPyNCP** and **NMe-pPyNCP** stem from the confused pyrrole rings in the macrocycle.

Introduction

Among biologically active aromatic compounds, cationic porphyrins and their metal complexes have attracted particular attention because of their remarkable affinity with double stranded DNA (dsDNA)[1–9] as well as the ability to cleave DNA.[10–16] 5,10,15,20-Tetrakis(4′-*N*-methylpyridyl)porphyrin (**TMPyP**, Chart 1) is a representative molecule of such cationic porphyrins. A number of studies on the interaction between **TMPyP** and dsDNA revealed several distinct binding modes (electrostatic binding along the outside of the DNA helix, groove binding, and intercalation), which depend on the buffer conditions and DNA sequences.[1–3,9,17] These studies have provided a framework for understanding the interactions between cationic porphyrins and dsDNA.

In parallel with the development of biological and diagnostic applications of cationic porphyrins, chemistry of porphyrinoids (porphyrin analogues) is expanding rapidly.[18] Porphyrinoids include porphyrin-like macrocycles with increased or reduced number of pyrrole units,[19–21] porphyrin-like tetrapyrroles possessing various heteroatoms in place of original carbon or nitrogen atoms,[22,23] and genuine isomers of porphyrin such as porphycene[24] or N-confused porphyrin.[25,26] It is highly plausible that some of these porphyrinoids have biological activities distinct from regular porphyrins.[27] However, only few have been decorated with cationic substituents for the study of their biological properties.[28–30]

N-Confused porphyrin (NCP, Chart 1) is one of the most attractive porphyrinoids due to the peculiar properties arising from a "*confused*" (*i.e.*, α,β′-linked) pyrrole ring in the macrocyclic core.[31,32] This structural feature forces one pyrrolic nitrogen atom to face outside of the macrocycle but this outward-pointing nitrogen can still participate in NH tautomerism, affording two types of tautomers (Chart 1).[33] In the macrocycle core of NCP, an internally protonated tautomer (3H-tautomer) has three hydrogen atoms whereas an externally protonated tautomer (2H-tautomer) has only two hydrogen atoms. At the peripheral nitrogen moiety, the 3H-tautomer can serve as a monodentate ligand for various metal ions whereas the 2H-tautomer recognizes neutral and anionic molecules through hydrogen bonding interactions.[25,26] These features associated with the outward-pointing nitrogen and its NH tautomerism would provide new advantages in the application for biological system. As a first step to exploit bioorganic chemistry of N-confused porphyrins in aqueous media, we have synthesized water soluble NCP and its *N*-methyl derivative and characterized their acid–base properties and DNA-binding abilities.

Results and discussion

Synthesis of cationic NCP and NMe-NCP

As a prototype of cationic porphyrin, we selected 5,10,15,20-tetrakis(α-pyridino-*p*-tolyl)porphyrin (**pPyP**, Chart 1) because it is reported to bind to dsDNA with an affinity comparable to that between **TMPyP** and dsDNA.[7] At first, a key precursor, 5,10,15,20-tetrakis(4′-bromomethylphenyl) NCP (**2**), was synthesized by one-pot condensation of pyrrole and *p*-bromomethylbenzaldehyde (**1**) with methanesulfonic acid (MSA), followed by oxidation with 2,3-dichloro-5,6-dicyano-*p*-benzoquinone (DDQ) (Scheme 1).[34] Compound **2** was then treated with excess pyridine to afford the target compound (**pPyNCP**).[7,35] The *N*(2)-methylated derivative of **pPyNCP** (**NMe-pPyNCP**) was also synthesized from **2** through selective methylation of peripheral nitrogen and then treatment with excess pyridine.[36]

Solubility of porphyrins and porphyrinoids in water was examined by partition experiments between ultrapure water

[a]*Department of Chemistry and Biochemistry, Graduate School of Engineering, Kyushu University, 744 Moto-oka, Nishi-ku, Fukuoka 819-0395, Japan. E-mail: hfuruta@cstf.kyushu-u.ac.jp; Fax: +81-92-802-2865*
[b]*Precursory Research for Embryonic Science and Technology (PRESTO), Japan Science and Technology Agency, Kawaguchi, Saitama 332-0012, Japan*

† Electronic supplementary information (ESI) available: Absorption, fluorescence, and CD spectra of water-soluble N-confused porphyrins in the titration and DNA binding experiments. See DOI: 10.1039/b810171j

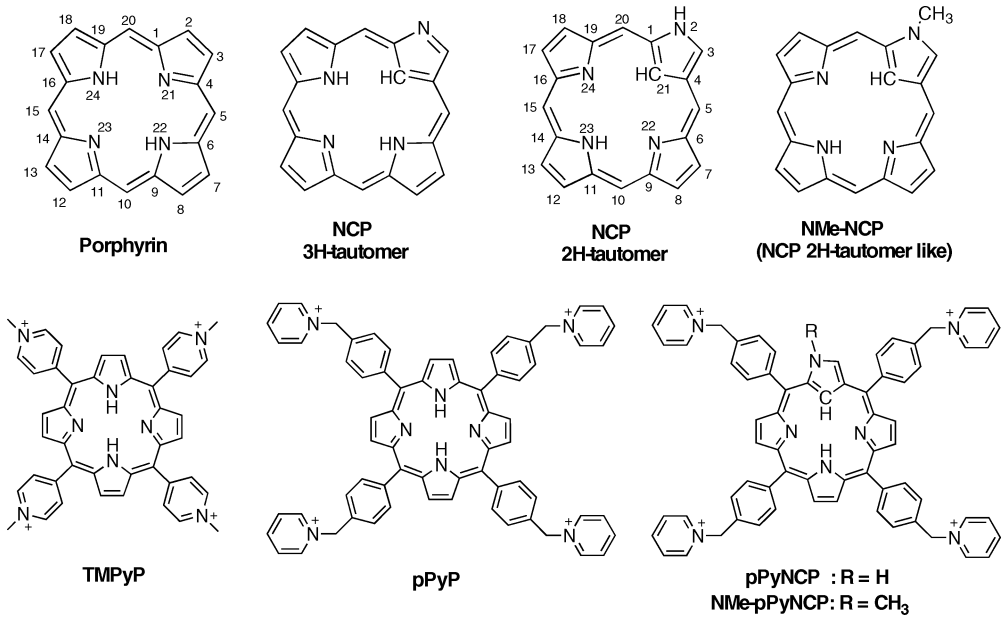

Chart 1 Porphyrin and N-confused porphyrins; (top) core structures of porphyrin, N-confused porphyrin, and *N*-methyl N-confused porphyrin, (bottom) structures of cationic porphyrins and its N-confused derivatives employed in this study.

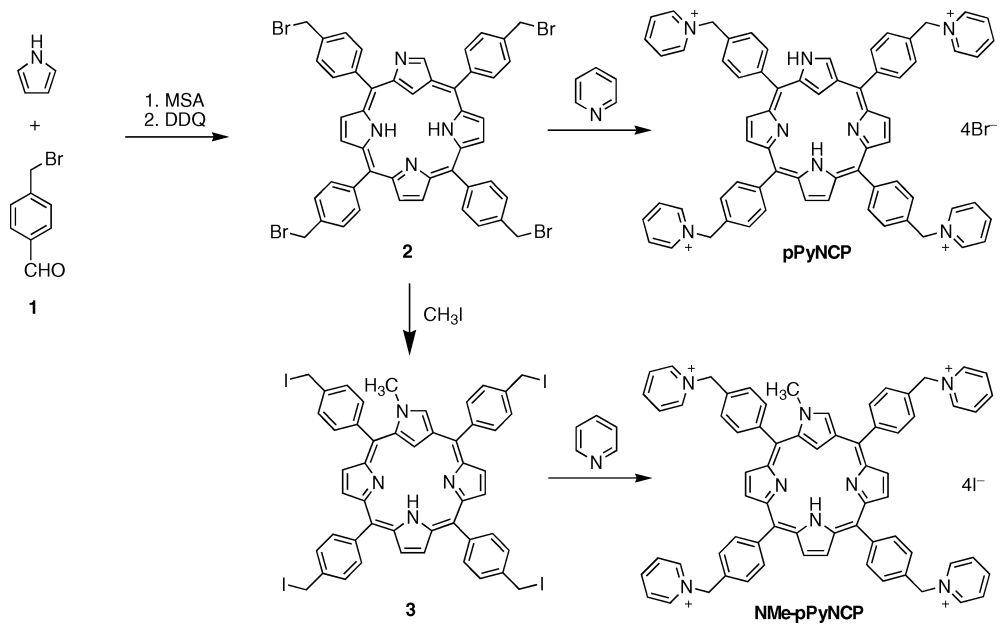

Scheme 1 Synthesis of **pPyNCP** and **NMe-pPyNCP**.

and CH_2Cl_2. 5,10,15,20-Tetraphenylporphyrin (TPP), 5,10,15,20-tetraphenyl-2-aza-21-carbaporphyrin (NCTPP), and 2-*N*-methyl-5,10,15,20-tetraphenyl-2-aza-21-carbaporphyrin (NMe-NCTPP) were extracted in CH_2Cl_2 phase (Fig. 1, lane b). In contrast, **pPyP**, **pPyNCP**, and **NMe-pPyNCP** were extracted in water phase (Fig. 1, lane c).

Molar extinction coefficients of **pPyP**, **pPyNCP**, and **NMe-pPyNCP** were determined in 50 mM HEPES buffer at pH 7.0 and 8.5 (Table 1). Over the concentration range (0.5–7.5 μM) examined, the absorption intensities of above compounds were linearly correlated to the concentrations of porphyrinoids without the shift of absorption maxima, which indicates that the aggregation of porphyrins is not significant under these buffer conditions.

Table 1 Absorption maxima (λ_{max}) and molar extinction coefficients (ε)

	pH 7.0		pH 8.5	
	λ_{max}/nm	$\varepsilon \times 10^5$	λ_{max} (nm)	$\varepsilon \times 10^5$
pPyP	416	3.48	415	2.63
pPyNCP	444	1.09	442	0.94
NMe-pPyNCP	460	0.88	448	0.84

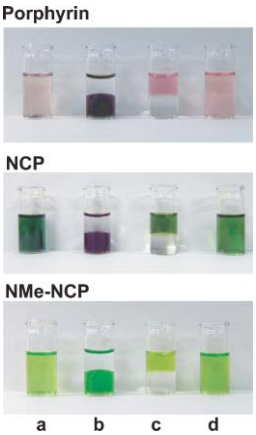

Fig. 1 Partition experiments of hydrophobic and hydrophilic derivatives of porphyrin (top), NCP (middle), and *N*-methyl NCP (bottom). Hydrophobic derivatives were dissolved in DMF (a) or H_2O + CH_2Cl_2 (b) and hydrophilic derivatives were dissolved in H_2O + CH_2Cl_2 (c) or DMF (d). Concentrations of porphyrins, NCPs, and *N*-methyl NCPs are 100 μM, 10 μM, and 10 μM, respectively.

Acid–base properties of pPyP

To access acid–base properties of cationic porphyrins (**pPyP**, **pPyNCP**, and **NMe-pPyNCP**) in aqueous solutions, UV-vis absorption spectra were measured under different ionic strength conditions. The low ionic strength was attained by adjusting the pH using HCl or NaOH without salt addition (Fig. 2). On the other hand, the high ionic strength was maintained by 0.2 M $NaNO_3$ and the pH was adjusted with HNO_3 or NaOH (Fig. S1).

pPyP exhibits a Soret band at 414 nm in neutral to basic pH range (Fig. 2A) and at 435 nm in acidic region (Fig. 2B). Each absorption maxima (λ_{max}) falls within the typical values of free-bases and dications of water-soluble *meso*-tetraaryl porphyrins.[6,7,37–39] In the pH 7.0 solution where **pPyP** takes a free-base form, **pPyP** exists as a mixture of monomer (λ_{max} = 414 nm) and *J*-aggregates (λ_{max} = 420 nm).[7] The ratio of these two forms is shown to be dependent on the buffer composition and **pPyP** concentration.[7,35,40,41] Under our conditions, **pPyP** exhibits a Soret band at 414 nm without a particular shoulder (Fig. 2A). The same trend is also observed under high ionic strength conditions (Fig. S1). These data indicate **pPyP** exists dominantly in a monomeric state at pH 7.0 and 8.5.

Generally, the equilibrium for the multistep proton dissociation process of porphyrin can be described by four dissociation constants (pK_{1-4}, Scheme 2).[42] However, detection of unstable porphyrin monocations is often difficult and the apparent dissociation constant (pK_a) between the free-base and dication has been employed as a convenient parameter (Scheme 2).[5,38,43] The apparent pK_a values of **pPyP** under the low and high ionic strength conditions were determined to be 3.5 and 4.3, respectively.

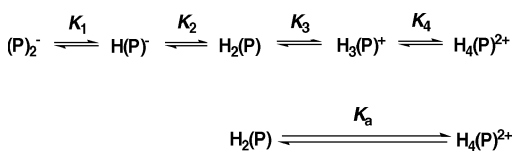

Scheme 2 Proton dissociation equilibria of porphyrin macrocycle.

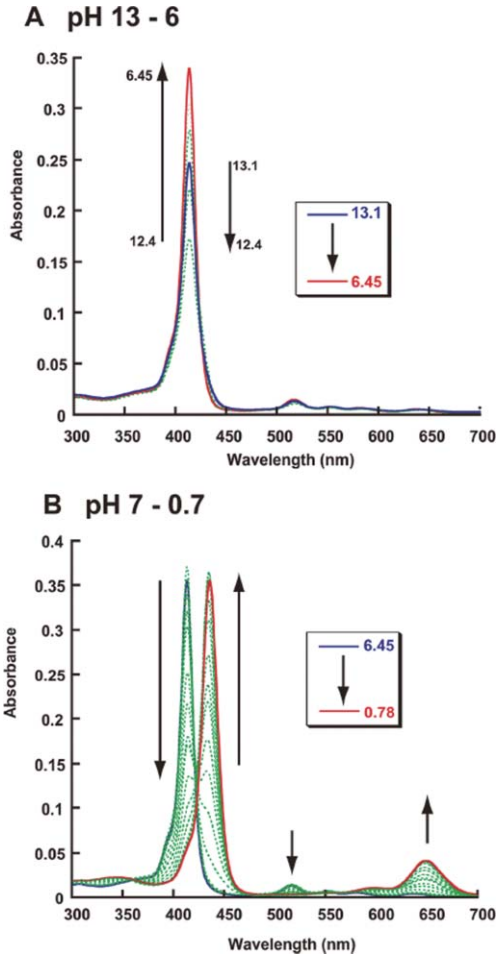

Fig. 2 Absorption spectra of **pPyP** (5 μM) titrated with NaOH and HCl; (A) pH 13–6 and (B) pH 7–0.7.

Acid–base properties of NMe-pPyNCP

In the pH titration of **NMe-pPyNCP** with HCl and NaOH, characteristic spectral changes were observed as follows: i) along with a pH decrease from 13 to 9, the intensity of the Soret band increased slightly without a shift of λ_{max} (446 nm) (Fig. 3A); ii) along with a pH decrease from 10 to 5, the intensity of the Soret band increased, coinciding with a red-shift of the λ_{max} by a 15 nm (446 to 461 nm). Q-type bands also showed a spectral change with an isosbestic point at 738 nm (Fig. 3B); iii) along with a pH decrease from 6 to 0.9, the intensity of the Soret band increased with a very small red-shift (461 to 463 nm) accompanied by a change of Q-type bands with new isosbestic points at 391 and 837 nm (Fig. 3C).

Through the comparison with the absorption spectra of the monocation and dication of NMe-NCTPP generated by the addition of trifluoroacetic acid in CH_2Cl_2 solution,[36] the major species formed at pH 5.6 and 0.91 can be identified as the monocation and dication of **NMe-pPyNCP**, respectively. Therefore, equilibrium constants between the species of dication and monocation (pK_4) and between monocation and free-base (pK_3) were estimated to be 4.2 and 8.6, respectively (Table 2). Similarly, from the pH titration under high ionic strength conditions (Fig. S1), pK_4 and pK_3 were estimated to be 4.5 and 8.6, respectively (Table 2).

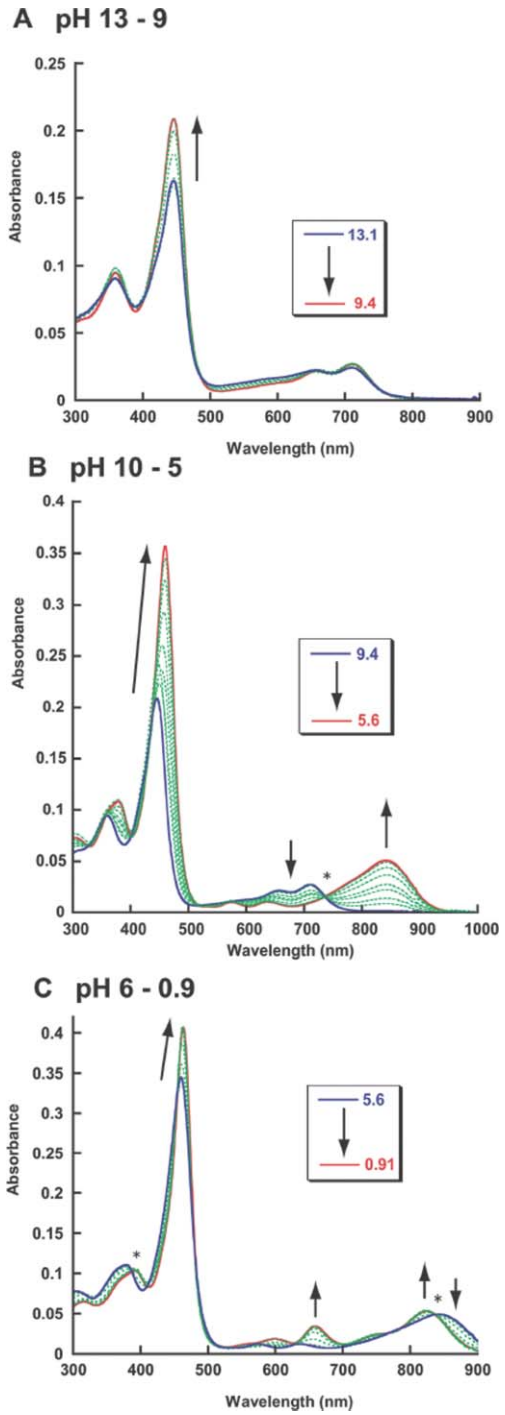

Fig. 3 Absorption spectra of **NMe-pPyNCP** (5 μM) titrated with NaOH and HCl; (A) pH 13–9, (B) pH 10–5, and (C) pH 6–0.9. Asterisk indicates isosbestic point.

Table 2 pK_{1-4} values of cationic N-confused porphyrins

	NMe-pPyNCP		**pPyNCP**		
Ionic strength	pK_4	pK_3	pK_4	pK_3	pK_2
Low	4.2	8.6	2.2	6.3	9.8
High	4.5	8.6	3.3	7.2	11.2

Acid–base properties of pPyNCP

In the pH titration of **pPyNCP** under low ionic strength conditions (Figs. 4A–C), spectral changes were seen at three pH regions (12–8.5, 8.5–4, and 4–1.8). In the neutral to acidic pH regions, the titration profile was similar to that of **NMe-pPyNCP** although the isosbestic points were less clear (Figs. 4B and 4C). However, at the basic pH region, further spectral change was observed with two isosbestic points at 622 and 698 nm (Fig. 4A). This change could be attributed to an equilibrium between the monoanion and free-base of **pPyNCP**. From the titration data, pK_4, pK_3, and pK_2 values were estimated to be 2.2, 6.3, and 9.8, respectively (Table 2). In a 2.5% aqueous micellar sodium dodecyl sulfate (SDS) solution, pK_4 and pK_3 values of NCTPP are reported to be 3.3 and 8.4, respectively.[31] Therefore, **pPyNCP** under low ionic strength conditions is less basic than NCTTP in aqueous micellar SDS. On the other hand, in the pH titration under high ionic strength conditions (Figs. 4D–F), spectral changes of **pPyNCP** were similar but not identical to those of low ionic strength conditions. Especially the changes in the Soret region were considerably different. pK_4, pK_3, and pK_2 were estimated to be 3.3, 7.2, and 11.2, respectively, which are one unit larger than the corresponding values obtained under the low ionic strength conditions (Table 2).

Interaction with double stranded DNA

Interaction between cationic N-confused porphyrins and dsDNA is an interesting issue because dsDNA binding ability is the most notable feature of cationic porphyrins.[1-9] Thus DNA titration experiments were carried out at pH 7.0 and 8.5 where the equilibrium of protonation is different in **pPyNCP** and **NMe-pPyNCP**. Namely, at pH 7.0, **pPyNCP** exists as a mixture of free–base and monocation whereas **NMe-pPyNCP** exists as monocation, predominantly. At pH 8.5, on the other hand, the free-base form is predominant with **pPyNCP** whereas **NMe-pPyNCP** exists as a mixture of free-base and monocation (Table 2).

In the presence of dsDNA from salmon testes at pH 7.0 or 8.5, **pPyP** shows a Soret band at 419 or 421 nm, respectively (Figs. 5A and S2). A positive circular dichroism (CD) signal was also induced in the Soret region (Fig. 5B). These results are consistent with a previous report concluding that **pPyP** interacts along the exterior of DNA helix.[7,41] UV-vis absorption and fluorescence spectra of **pPyP** were not drastically changed by the addition of dsDNA (Fig. 5), which suggests that the porphyrin core of **pPyP** received no significant perturbation from dsDNA.[37,44]

Then we examined the interaction between dsDNA and **NMe-pPyNCP** (Fig. 6). Both at pH 7.0 and 8.5, addition of dsDNA induced red-shifts of the Soret band to 464–465 nm, accompanied by the increase of Q-like band at 809–810 nm (Fig. 6A and 6D). These changes were closely similar to those observed in the formation of **NMe-pPyNCP** dication, which shows the Soret band at 464 nm and an intensified Q-like band at 823 nm (Figs. 4C and S1). This similarity strongly suggests that the interaction of **NMe-pPyNCP** and dsDNA induces the formation of **NMe-pPyNCP** dication at 7.0 (Fig. 6D) and even at pH 8.5 (Fig. S3). Addition of dsDNA significantly enhanced the fluorescent from **NMe-pPyNCP** (Fig. 6C). This result also suggests the dication

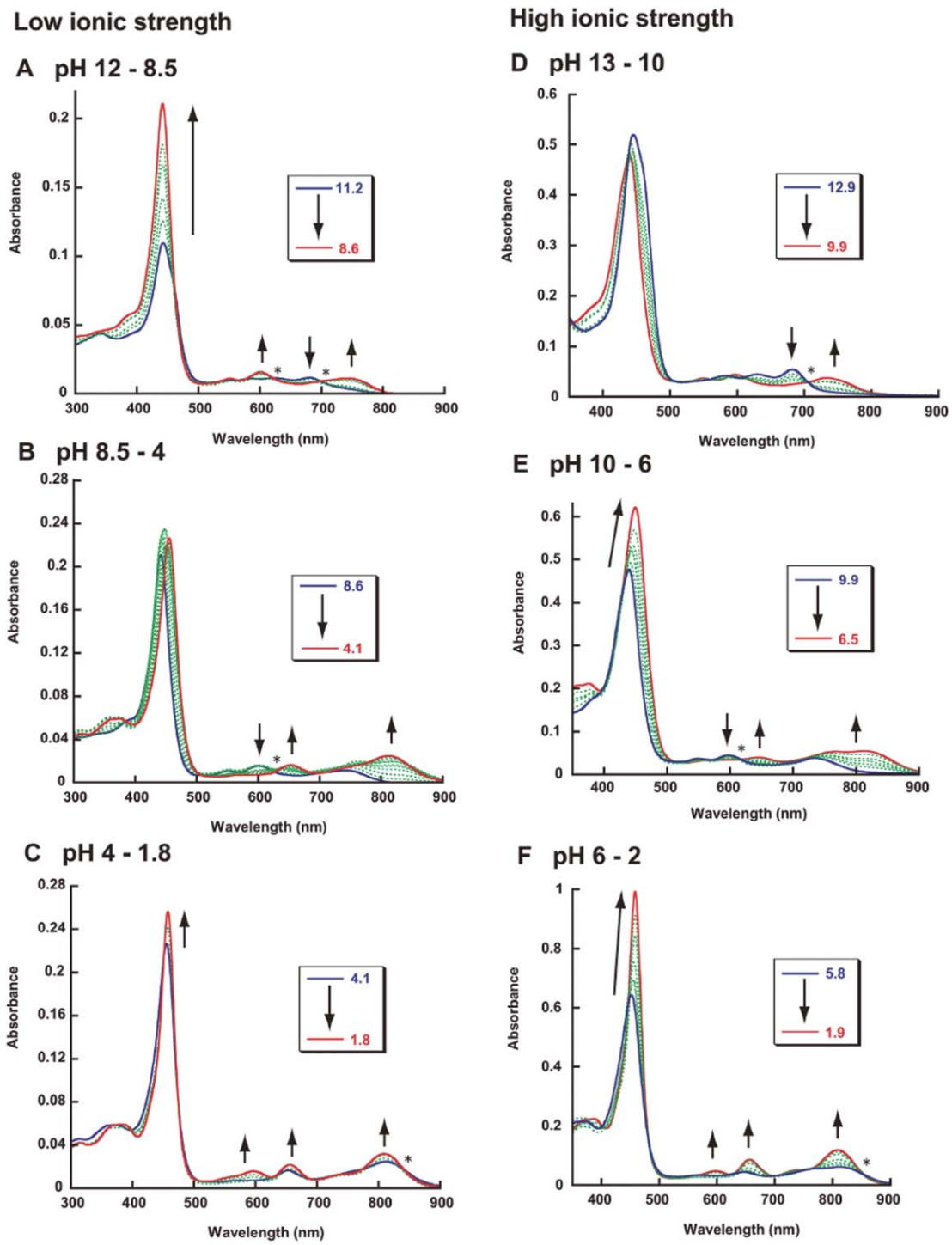

Fig. 4 pH dependence of absorption spectra of **pPyNCP**. A–C: pH was adjusted with NaOH and HCl; (A) pH 12–8.5, (B) pH 8.5–4, and (C) pH 4–1.8. D–F: pH was adjusted with NaOH and HNO_3 in the presence of 0.2 M $NaNO_3$; (D) pH 13–10, (E) pH 10–6, and (F) pH 6–2. Asterisk indicates isosbestic point. [**pPyNCP**] = 5 μM.

formation because similar fluorescent enhancement was observed by protonation of **NMe-pPyNCP** (Fig. S4).

In the UV-vis spectra at pH 7.0, the titration of **NMe-pPyNCP** with dsDNA exhibited an isosbestic point at 838 nm (Fig. 6A), which is almost identical with that observed in the transition between the monocation and dication (837 nm). Whereas the pK_4 of **NMe-pPyNCP** is 4.2 or 4.5 (Table 2), the above result suggests that dsDNA induced a transition of the **NMe-pPyNCP** monocation to the dication at pH 7.0. At pH 8.5 where **NMe-pPyNCP** exists as a mixture of free base and monocation,

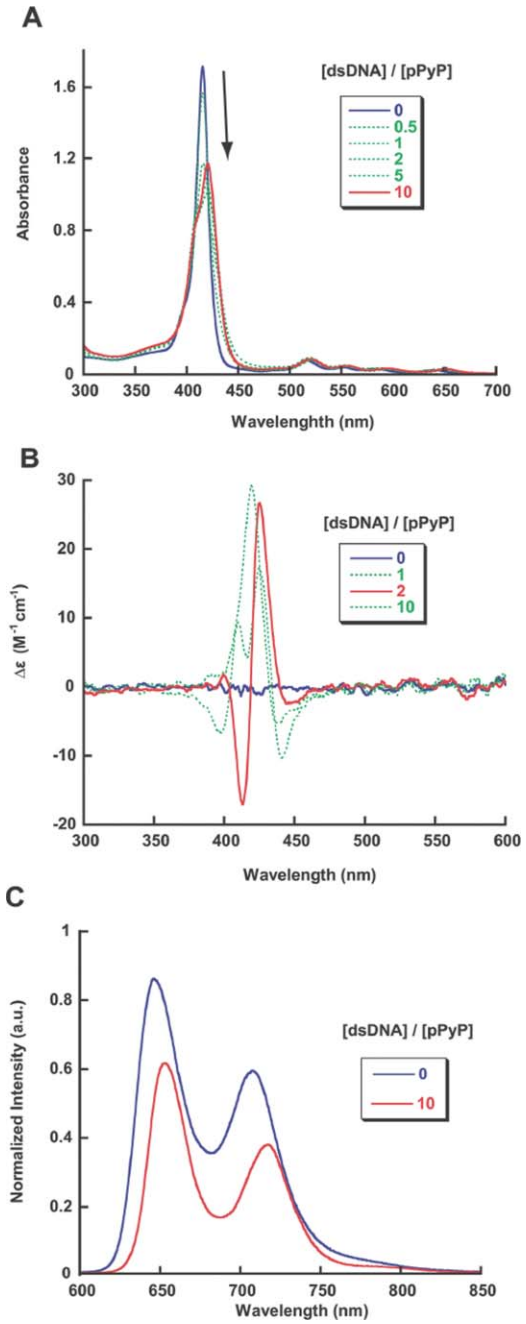

Fig. 5 Double stranded DNA binding ability of **pPyP**. A: Absorption spectra of **pPyP** (5 μM) in the absence and presence of dsDNA at pH 7.0. B: Circular dichroism spectra of **pPyP** (5 μM) in the absence and presence of dsDNA at pH 7.0. C: Fluorescence spectra of **pPyP** in the absence and presence of dsDNA at pH 7.0. Excited at 414 nm in the absence of dsDNA and at 421 nm in the presence of dsDNA.

addition of the dsDNA gave the isosbestic point at 741 nm (Fig. 6D), which suggests that **NMe-pPyNCP** binds to the dsDNA without affecting its own equilibrium between the free-base and monocation under the present conditions.

Association between **NMe-pPyNCP** and dsDNA was also supported by the positive CD signal in the Soret region (Fig. 6B). At pH 7.0, induced CD spectra showed two isosbestic points at 336 and 409 nm. Closely similar CD spectra were also observed

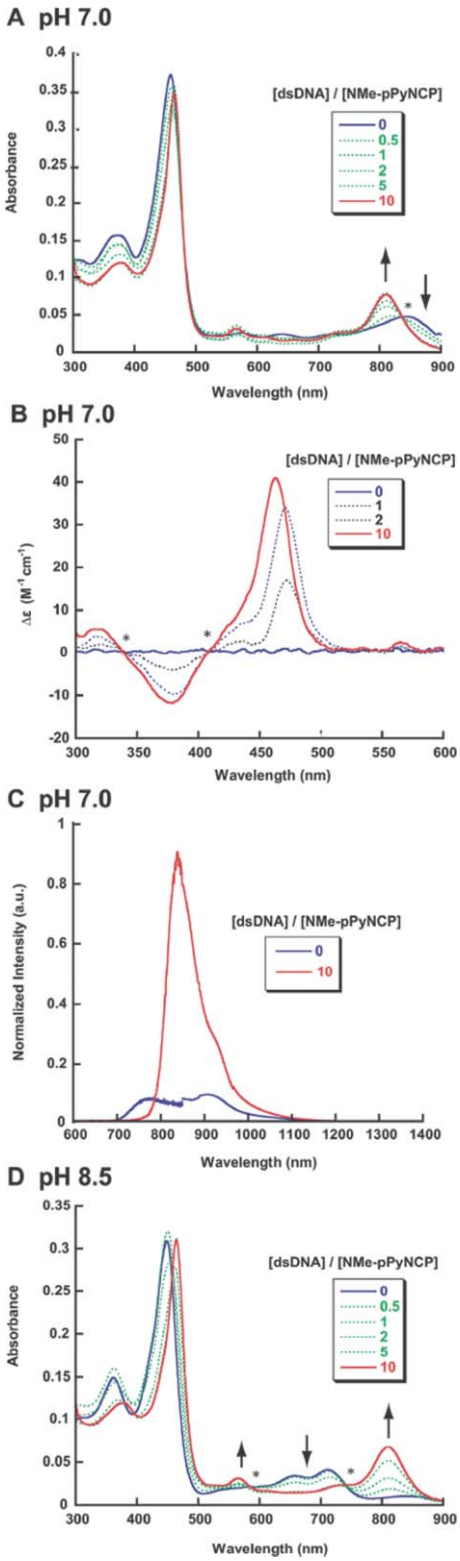

Fig. 6 Double stranded DNA binding ability of **NMe-pPyNCP**. A: Absorption spectra of **NMe-pPyNCP** (5 μM) in the absence and presence of dsDNA at pH 7.0. B: Circular dichroism spectra of **NMe-pPyNCP** (15 μM) in the absence and presence of dsDNA at pH 7.0. C: Fluorescence spectra of **NMe-pPyNCP** in the absence and presence of dsDNA at pH 7.0. Excited at 444 nm in the absence of dsDNA and at 464 nm in the presence of dsDNA. D: Absorption spectra of **NMe-pPyNCP** (5 μM) in the absence and presence of dsDNA at pH 8.5. Asterisk indicates isosbestic point.

even at pH 8.5 with two isosbestic points at 338 and 409 nm (Fig. S3), indicating that in both pH 7.0 and 8.5, binding mode between **NMe-pPyNCP** and dsDNA is basically unchanged. By analogy to the porphyrin–DNA interaction, the observed positive CD spectra suggest that **NMe-pPyNCP** binds to the phosphate backbones and/or helical grooves of dsDNA.[45]

Upon addition of dsDNA at pH 7.0, where **pPyNCP** exists as a mixture of free-base and monocation, **pPyNCP** showed a red-shift of the Soret band to 459 nm and a rise of Q-like band at 798 nm (Fig. 7A). These changes suggest a formation of NCP dication that exhibits the Soret and Q-like bands at 458 and 809 nm, respectively (Fig. 4C and 4F). Fluorescent spectra of **pPyNCP** were also significantly enhanced upon the addition of dsDNA (Fig. 7C) or acid (Fig. S4). Similar to the case of **NMe-pPyNCP**, protonation of **pPyNCP** was facilitated by the binding with dsDNA to form the dication at pH 7.0. In the titration at pH 8.5, however, only a small amount of dication is induced to form by the addition of dsDNA, presumably because **pPyNCP** is less basic than **NMe-pPyNCP** (Fig. 7D).

In the titrations of **pPyP** and **NMe-pPyNCP**, significant spectral changes were observed with one- and two-fold molar amounts of DNA base-pairs, respectively (Fig. 5A and 6A). On the other hand, spectral changes were modest for **pPyNCP** until adding a five-fold molar amount of DNA base-pairs (Fig. 7A). These results suggest that the affinity to dsDNA could be aligned in the order of **pPyP** > **NMe-pPyNCP** > **pPyNCP** at pH 7.0 although the precise comparison based on their DNA binding constants, which were not yet available due to the lack of isosbestic points with **pPyP** and **pPyNCP**, is an issue to be addressed. Acid dissociation constants in Scheme 2 provide an equation $pK_a = pK_3 + pK_4$, from which expected pK_a values of **pPyNCP** and **NMe-pPyNCP** can be calculated to be 8.5 and 12.8 under the low ionic strength conditions and 10.5 and 13.1 under the high ionic strength conditions, respectively. These values are much higher than those of **pPyP** that are 3.5 and 4.3 under the low and high ionic strength conditions, respectively. Therefore an order of pK_a values, **NMe-pPyNCP** > **pPyNCP** > **pPyP**, is not directly related to the order of apparent affinity to dsDNA.

Interaction with single stranded DNA

Interaction of cationic porphyrins with single stranded nucleic acids was less extensively investigated than that with dsDNA although a limited number of studies were performed with **TMPyP**.[45–47] We examined the effects of single stranded DNA (ssDNA) using a 20 nucleotide oligomer (5′-TGTAGGCATGCTTAAGCAT-3′). This sequence contains approximately equal number of four nucleobases and thus, is unlikely to form particular secondary structures.

Upon addition of the ssDNA, spectral changes of the UV-vis absorption of **pPyNCP** and **NMe-pPyNCP** were closely similar to those observed with dsDNA (Fig. S5). However, the induced CD spectra with ssDNA were different from those with dsDNA (Fig. 8). Consistent with the result of **TMPyP** with poly(dA), where the negative CD signals at the Soret regions are observed,[45] **pPyP** gave negative CD signals with ssDNA (Fig. 8A). On the other hand, **pPyNCP** exhibited positive CD spectra but their shapes were different from those induced by dsDNA (Fig. 8B). These results suggest that the helical structure of double

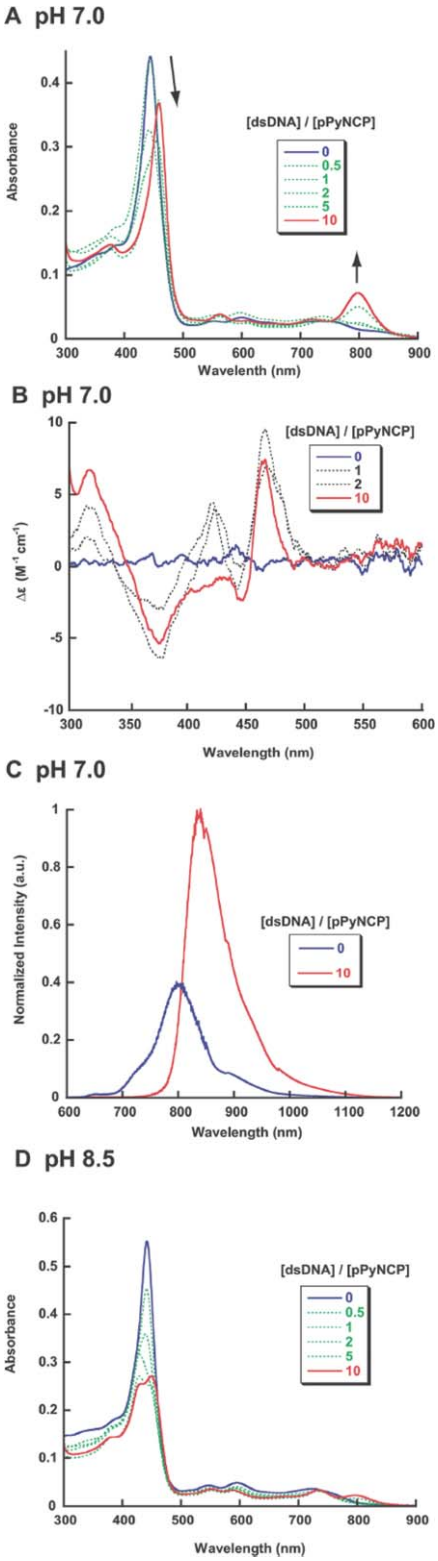

Fig. 7 Double stranded DNA binding ability of **pPyNCP**. A: Absorption spectra of **pPyNCP** (5 μM) in the absence and presence of dsDNA at pH 7.0. B: Circular dichroism spectra of **pPyNCP** (15 μM) in the absence and presence of dsDNA at pH 7.0. C: Fluorescence spectra of **pPyNCP** in the absence and presence of dsDNA at pH 7.0. Excited at 458 nm in the absence of dsDNA and at 464 nm in the presence of dsDNA. D: Absorption spectra of **pPyNCP** (5 μM) in the absence and presence of dsDNA at pH 8.5.

stranded DNA plays specific role in the interactions with **pPyP** and **pPyNCP**. In the case of **NMe-pPyNCP**, ss- and ds-DNA induced similar CD signals at the Soret region where the two isosbestic points were observed at 336 and 411 nm (Fig. 8C), which suggests that the binding mode(s) of **NMe-pPyNCP** with ss- and ds-DNA are closely similar.

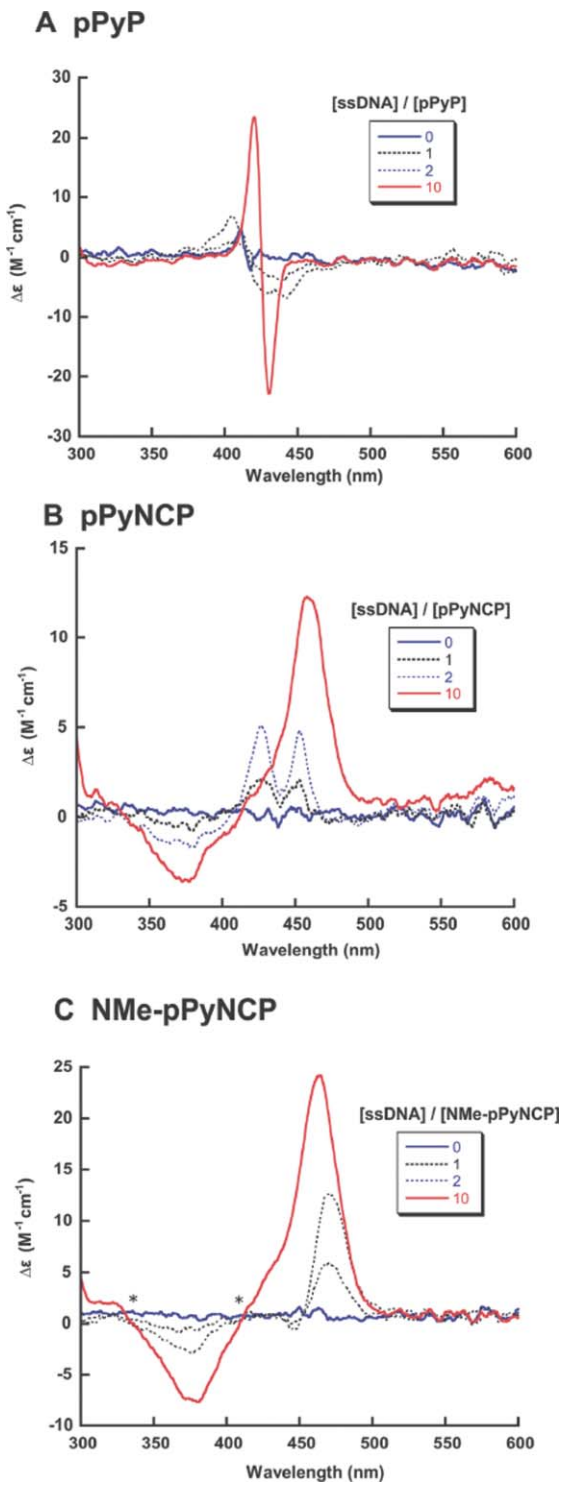

Fig. 8 Single stranded DNA binding ability of the cationic porphyrin and its confused derivatives. Circular dichroism spectra of 5 μM **pPyP** (A), 15 μM **pPyNCP** (B), and 15 μM **NMe-pPyNCP** (C) in the absence and presence of ssDNA at pH 7.0. Asterisk indicates isosbestic point.

Conclusions

We have synthesized water-soluble derivatives of NCP bearing cationic side-arms, **pPyNCP** and **NMe-pPyNCP**, and their pK_{1-4} values were determined in aqueous solution. Titration experiments with dsDNA revealed that, both **pPyNCP** and **NMe-pPyNCP** bind to dsDNA similar to the mother porphyrin **pPyP**, with affinity order of **pPyP** > **NMe-pPyNCP** > **pPyNCP**. Photophysical behaviors of **pPyNCP** were influenced by buffer compositions and DNA structures. This property might arise from the confused pyrrole moiety which can serve as proton/cation and anion binding sites depending on the tautomerism of NCP skeleton. On the other hand **NMe-pPyNCP** appears considerably robust against these factors. Interestingly, the fluorescence of **NMe-pPyNCP** was significantly enhanced by the addition of DNA, because of the induced formation of NMe-NCP dication by association. This features should be attributed to much higher basicity of the NMe-NCP skeleton than mother porphyrin macrocycle.

Recently quadraplex DNAs and functional RNAs receive significant attention as novel targets of cationic porphyrins and their related macrocycles.[28,48–51] Unlike simple DNA double helix, they have more complex structures consisting of canonical and noncanonical base-pairings as well as single stranded regions.[48,52] Therefore the robust DNA binding ability of **NMe-pPyNCP** revealed in this study might be attractive to develop novel molecules that can modulate and probe the structures and functions of quadraplex DNAs and functional RNAs that play pivotal roles in living cells.[48,52]

Besides DNA binding ability studied in this study, water soluble porphyrins have been known to have other interesting properties. For instance, self-aggregation of porphyrin macrocycle in aqueous media is typically observed in porphyrins with water-soluble neutral or anionic moieties.[38,53] Generation of singlet oxygen inside living cells is also an important property of porphyrins which makes them promising compounds as photosensitisers for photodynamic therapy.[54] To address these properties of N-confused porphyrins, we are currently synthesizing other types of water soluble NCPs bearing non-cationic hydrophilic moieties or exhibiting cell penetrating abilities.

Experimental

Chemicals

For chemical synthesis, commercially available reagents and solvents were used without further purification. Silica gel column chromatography was performed on KANTO Silica Gel 60 N (spherical, neutral, particle size 40–50 μm). For preparation of aqueous buffer solutions for photophysical measurements, molecular biology grade reagents (Nacalai Tesque, Kyoto, Japan) and ultrapure water (prepared by Organo Puric-Z, Tokyo, Japan) were employed. Double stranded DNA (dsDNA) from salmon testes and synthetic single stranded DNA (ssDNA) (5′-TGTAGGCATGCTTAAGCAT-3′) were purchased from Sigma-Aldrich Japan (Tokyo, Japan) and Hokkaido System Science

(Hokkaido, Japan), respectively. Concentrations of DNA solutions were calculated from absorbance at 260 nm. In DNA titration experiments, the molar ratios between the compounds and DNA were adjusted using the molar concentration of DNA base-pairs for dsDNA or with that of nucleobases for ssDNA, respectively.

Spectral measurements

^{1}H NMR spectra were recorded on a JEOL JNM-AL300 spectrometer (operating 300.40 MHz for ^{1}H). Chemical shifts were expressed in parts per million from a residual portion of deuterated solvent, $CHCl_3$ ($\delta = 7.26$). The chemical shift of HDO at a given temperature was determined by the previously reported equation. UV-Vis, fluorescence, and CD spectra were measured using 10 mm quartz cells (except for CD spectra of **pPyP** for which 20 mm quartz cell was used) at ambient temperature. UV-vis spectra were recorded on a Shimadzu UV-3150PC spectrometer using 5 μM solutions. Induced CD spectra, which were recorded on a JASCO J-720 spectropolarimeter, were obtained as averages of three accumulations recorded with steps of 0.5 nm (band width: 2.0 nm, response: 2 s, scan speed: 200 nm min^{-1}) using 5 μM **pPyP** solutions or 15 μM **pPyNCP** and **NMe-pPyNCP** solutions. Fluorescence spectra were recorded on an SPEX Fluorolog spectrometer (HORIBA) with photomultiplier module (Hamamatsu R928P) and InGaAs photodiode array. Excitation wavelengths, which were set at the absorption maxima of the Soret bands of respective sample solutions, are shown in the figure legends. Intensities of absorption spectra of respective sample solutions were adjusted to be 0.1 and relative intensities of fluorescence spectra were normalized with molar extinction coefficients at the excitation wavelengths.

Synthesis

5,10,15,20-Tetrakis(4′-bromomethylphenyl)-2-aza-21-carbaporphyrin (2)

Pyrrole (0.69 mL, 10 mmol) and **1** (1.99 g, 10 mmol) were dissolved in 1 L of CH_2Cl_2 and the reaction was initiated by adding methanesulfonic acid (MSA) (0.45 mL, 7 mmol). The reaction mixture, which soon turned dark brown, was stirred at room temperature for 30 min. 2,3-Dichloro-5,6-dicyano-*p*-benzoquinone (DDQ) (2.00 g, 8.8 mmol) was added and the mixture was allowed to stir for 1 min and then the reaction was quenched by adding water saturated with Na_2CO_3. The organic layer was separated and the solution was dried over Na_2SO_4. The solution was purified by silica gel column chromatography with CH_2Cl_2–CH_3OH (v/v = 100 : 3) as eluants and precipitated from CH_2Cl_2–CH_3OH. **2** was obtained as dark green solid, which was subjected for subsequent transformations as quickly as possible after precipitation without drying because **2** was unstable under condensed conditions. ^{1}H NMR ($CDCl_3$, ppm): δ −5.04 (s, 1H), 4.80 (s, 2H), 4.82 (s, 6H), 7.77 (d, 4H, $J = 7.2$ Hz), 7.85–7.87 (m, 4H), 8.11 (d, 2H, $J = 6.6$ Hz), 8.13 (d, 2H, $J = 6.9$ Hz), 8.29 (d, 1H, $J = 7.8$ Hz), 8.34 (d, 2H, $J = 8.1$ Hz), 8.53–8.56 (m, 3H), 8.61 (d, 2H, $J = 4.2$ Hz), 8.70 (s, 1H), 8.93 (d, 1H, $J = 4.8$ Hz), 8.98 (d, 1H, $J = 5.7$ Hz).

5,10,15,20-Tetrakis(α-pyridinio-*p*-tolyl)-2-aza-21-carbaporphyrin tetrabromide salt (pPyNCP)

Compound **2** was prepared from 10 mmol pyrrole and 10 mmol aldehyde and was employed directly after precipitation without drying. **2** was dissolved in 500 mL of pyridine. The mixture was vigorously stirred for 7 days at ambient temperature. The solution was filtrated. A dark green solid of **pPyNCP** was obtained as a hygroscopic solid in 7.8% yield from **1** (276 mg, 194 μmol as $7H_2O$ adduct). ^{1}H NMR (D_2O, 80 °C): δ 6.18 (s, 4H), 6.20 (s, 4H), 7.85–7.93 (m, 9H), 8.13–8.14 (m, 9H), 8.27 (m, 11H), 8.39–8.41 (m, 2H), 8.53 (s, 2H), 8.57 (s, 2H), 8.65 (s, 1H), 8.72 (m, 4H), 9.18 (d, 8H, $J = 6.0$ Hz). [Note: inner C(21)H, which was not observed in D_2O due to H-D exchange, was observed in DMSO-d_6 at δ 0.46 (s, 1H)]. Anal. Calcd for $C_{68}H_{55}N_8Br_4 \cdot 7H_2O$: C: 57.16, H: 4.80, N: 7.84, found: C: 57.10, H: 4.73, N: 7.83%.

2-*N*-Methyl-5,10,15,20-tetrakis(4′-iodomethylphenyl)-2-aza-21-carbaporphyrin (3)

Compound **2** prepared from 3 mmol pyrrole and 3 mmol aldehyde was employed directly after precipitation without drying. **2** was dissolved in 300 mL of CH_2Cl_2. To the solution, 20 mL of iodomethane was added. The reaction mixture was stirred for 15 h at ambient temperature. After the reaction was completed, the solvent was evaporated and the residue was purified on a silica gel column with CH_2Cl_2–CH_3OH (v/v = 100 : 3) as eluants. The dark green fraction was collected and the solvent was evaporated to afford **3** in 5.0% yield from **1** (37.5 mg, 37.7 μmol). ^{1}H NMR ($CDCl_3$): δ 1.09 (s, 1H), 3.39 (s, 3H), 4.67 (s, 8H), 7.10 (s, 1H), 7.45 (d, 1H, $J = 4.5$ Hz), 7.48 (d, 1H, $J = 4.5$ Hz), 7.56–7.67 (m, 8H), 7.71–7.74 (m, 6H), 7.80–7.91 (m, 6H).

2-*N*-Methyl-5,10,15,20-tetrakis(α-pyridinio-*p*-tolyl)-2-aza-21-carbaporphyrin tetraiodide salt (NMe-pPyNCP)

37.5 mg (37.7 μmol) of **3** was dissolved in pyridine and vigorously stirred for 6 days at room temperature. After the solution was filtrated, the residue was dried to afford **NMe-pPyNCP** (31.1 mg, 16.3 μmol as 1(pyridine)·2HI·$2H_2O$ adduct) as a hygroscopic solid in 43% yield. ^{1}H NMR (D_2O, 80 °C): δ −0.10 (s, 1H), 3.47 (s, 3H), 6.10 (s, 4H), 6.12 (s, 2H), 6.13 (s, 1H), 7.55 (d, 1H, $J = 5.1$ Hz), 7.60 (d, 1H, $J = 4.6$ Hz), 7.69 (s, 1H), 7.75–7.82 (m, 8H), 7.87–7.93 (m, 5H), 7.98–8.00 (m, 7H), 8.21–8.27 (m, 8H), 8.69 (d, 2H, $J = 7.8$ Hz), 8.74 (d, 2H, $J = 8.1$ Hz), 9.11 (d, 8H, $J = 5.1$ Hz). Anal. Calcd for $C_{69}H_{56}N_8I_4 \cdot C_5H_5N_1 \cdot 2HI \cdot 2H_2O$: C: 46.49, H: 3.74, N: 6.59, found: C: 47.08, H: 3.63, N: 6.74%.

5,10,15,20-Tetrakis(α-pyridinio-*p*-tolyl)porphyrin tetrabromide salt (pPyP)

5,10,15,20-Tetrakis(4′-bromomethylphenyl)porphyrin (18.5 mg, 18.8 μmol) was dissolved in 20 mL of pyridine and the solution was refluxed for 2 h with vigorous stirring. After the solvent was filtrated, **pPyP** was obtained as a purple solid in 81% yield (20.6 mg, 15.3 μmol as $2H_2O$ adduct). ^{1}H NMR (DMSO-d_6): δ −3.03 (s, 2H, inner NH), 6.23 (s, 8H, -CH_2-), 7.95 (d, 8H, $J =$ 8.4 Hz, phenyl), 8.27 (d, 8H, $J = 7.8$ Hz, phenyl), 8.35 (t, 8H, $J =$ 7.1 Hz, pyridine), 8.77 (t, 4H, $J = 8.1$ Hz, pyridine), 8.78 (s, 8H, β pyrrole), 9.48 (d, 8H, $J = 5.7$ Hz, pyridine), ^{1}H NMR (D_2O,

80 °C): δ 6.62 (s, 8H, -CH_2-), 8.32 (d, 8H, $J = 7.3$ Hz, phenyl), 8.69 (t, 8H, $J = 6.7$ Hz, pyridine), 8.75 (d, 8H, $J = 7.9$ Hz, phenyl), 9.15 (t, 4H, $J = 7.6$ Hz, pyridine), 9.39 (s, 8H, β-pyrrole), 9.60 (d, 8H, $J = 6.1$ Hz, pyridine). Anal. Calcd for $C_{68}H_{55}N_8Br_4 \cdot 2H_2O$: C: 60.96, H: 4.44, N: 8.36, found: C: 60.75, H: 4.20, N: 8.30%.

Acknowledgements

We acknowledge Dr Kazuki Sada for the help with measurements of CD spectra. This work was partly supported by Grant-in-Aids for Young Scientists (A) (No. 18685020 to Y.I.), Exploratory Research (No. 19657071 to Y.I.), and the Global COE program, "Science for Future Molecular Systems" (to H.F.) from the Ministry of Education, Culture, Sports, Science and Technology of Japan.

References

1 R. J. Fiel, J. C. Howard, E. H. Mark and N. Datta-Gupta, *Nucleic Acids Res.*, 1979, **6**, 3093–3118.
2 R. J. Fiel, *J. Biomol. Struct. Dyn.*, 1989, **6**, 1259–1274.
3 L. G. Marzilli, *New J. Chem.*, 1990, **14**, 409–420.
4 N. Robic, C. Bied-Charreton, M. Perrée-Fauvet, C. Verchère-Béaur, L. Salmon, A. Gaudemer and R. F. Pasternack, *Tetrahedron Lett.*, 1990, **31**, 4739–4742.
5 L. G. Marzilli, G. Pethö, M. Lin, M. S. Kim and D. W. Dixon, *J. Am. Chem. Soc.*, 1992, **114**, 7575–7577.
6 J. E. McClure, L. Baudouin, D. Mansuy and L. G. Marzilli, *Biopolymers*, 1997, **42**, 203–217.
7 P. Kubát, K. Lang, P. Anzenbacher Jr., K. Jursíková, V. Král and B. Ehrenberg, *J. Chem. Soc., Perkin Trans. 1*, 2000, 933–941.
8 D. H. Tjahjono, T. Yamamoto, S. Ichimoto, N. Yoshioka and H. Inoue, *J. Chem. Soc., Perkin Trans. 1*, 2000, 3077–3081.
9 D. R. McMillin, A. H. Shelton, S. A. Bejune, P. E. Fanwick and R. K. Wall, *Coord. Chem. Rev.*, 2005, **249**, 1451–1459.
10 R. J. Fiel, T. A. Beerman, E. H. Mark and N. Datta-Gupta, *Biochem. Biophys. Res. Commun.*, 1982, **107**, 1067–1074.
11 D. Praseuth, A. Gaudemer, J. B. Verlhac, I. Kraljic, I. Sissoëff and E. Guillé, *Photochem. Photobiol.*, 1986, **44**, 717–724.
12 B. Ward, A. Skorobogaty and J. C. Dabrowiak, *Biochemistry*, 1986, **25**, 6875–6883.
13 J. T. Groves and T. P. Farrell, *J. Am. Chem. Soc.*, 1989, **111**, 4998–5000.
14 S. R. Chatterjee, S. J. Shetty, T. P. Devasagayam and T. S. Srivastava, *J. Photochem. Photobiol., B*, 1997, **41**, 128–135.
15 S. Mettath, B. R. Munson and R. K. Pandey, *Bioconjugate Chem.*, 1999, **10**, 94–102.
16 S. Yellappa, J. Seetharamappa, L. M. Rogers, R. Chitta, R. P. Singhal and F. D'Souza, *Bioconjugate Chem.*, 2006, **17**, 1418–1425.
17 Y. H. Chae, B. Jin, J. K. Kim, S. W. Han, S. K. Kim and H. M. Lee, *Bull. Korean Chem. Soc.*, 2007, **28**, 2203–2208.
18 J. L. Sessler and S. J. Weghorn, *Expanded, Contracted & Isomeric Porphyrins*, Elsevier, Oxford 1997.
19 S. Shimizu and A. Osuka, *J. Porphyrins Phthalocyanines*, 2004, **8**, 175–181.
20 R. Misra and T. K. Chandrashekar, *Acc. Chem. Res.*, 2008, **41**, 265–279.
21 Y. Inokuma and A. Osuka, *Dalton Trans.*, 2008, 2517–2526.
22 P. J. Chmielewski and L. Latos-Grazyński, *Coord. Chem. Rev.*, 2005, **249**, 2510–2533.
23 I. Gupta and M. Ravikanth, *Coord. Chem. Rev.*, 2006, **250**, 468–518.
24 D. Sanchez-Garcia and J. L. Sessler, *Chem. Soc. Rev.*, 2008, **37**, 215–232.
25 H. Furuta, H. Maeda and A. Osuka, *Chem. Commun.*, 2002, 1795–1804.
26 H. Maeda and H. Furuta, *Pure Appl. Chem.*, 2006, **78**, 29–44.
27 V. Král, J. Králová, R. Kaplánek, T. Bríza and P. Martásek, *Physiol. Res.*, 2006, **55**, S3–S26.
28 J. Seenisamy, S. Bashyam, V. Gokhale, H. Vankayalapati, D. Sun, A. Siddiqui-Jain, N. Streiner, K. Shin-Ya, E. White, W. D. Wilson and L. H. Hurley, *J. Am. Chem. Soc.*, 2005, **127**, 2944–2959.
29 Z. Gershman, I. Goldberg and Z. Gross, *Angew. Chem., Int. Ed.*, 2007, **46**, 4320–4324.
30 A. K. Bordbar, M. Davari, E. Safaei and V. Mirkhani, *J. Porphyrins Phthalocyanines*, 2007, **11**, 139–147.
31 H. Furuta, T. Asano and T. Ogawa, *J. Am. Chem. Soc.*, 1994, **116**, 767–768.
32 P. J. Chmielewski, L. Latos-Grażyński, K. Rachlewicz and T. Głowiak, *Angew. Chem., Int. Ed. Engl.*, 1994, **33**, 779–781.
33 H. Furuta, T. Ishizuka, A. Osuka, H. Dejima, H. Nakagawa and Y. Ishikawa, *J. Am. Chem. Soc.*, 2001, **123**, 6207–6208.
34 G. R. Geier III, D. M. Haynes and J. S. Lindsey, *Org. Lett.*, 1999, **1**, 1455–1458.
35 T. Yamashita, T. Uno and Y. Ishikawa, *Bioorg. Med. Chem.*, 2005, **13**, 2423–2430.
36 P. J. Chmielewski and Latos-Grażyński, *J. Chem. Soc., Perkin Trans. 2*, 1995, 503–509.
37 N. E. Mukundan, G. Pethö, D. W. Dixon, M. S. Kim and L. G. Marzilli, *Inorg. Chem.*, 1994, **33**, 4676–4687.
38 N. C. Maiti, S. Mazumdar and N. Periasamy, *J. Phys. Chem. B*, 1998, **102**, 1528–1538.
39 I. Hanyz and D. Wróbel, *Photochem. Photobiol. Sci.*, 2002, **1**, 126–132.
40 K. Procházková, Z. Zelinger and P. Kubát, *J. Phys. Org. Chem.*, 2004, **17**, 890–897.
41 T. Yamashita, PhD Thesis, Kumamoto University, Kumamoto, 2005.
42 P. Hambright, in *Porphyrins and Metalloporphyrins*, ed. K. M. Smith, Elsevier, Amsterdam, 1975, pp. 234–238.
43 K. Kalyasundaram, *Photochemistry of Polypyridine and Porphyrin Complexes*, Academic Press, London, 1992.
44 G. Pethö, N. B. Elliott, M. S. Kim, M. Lin, D. W. Dixon and L. G. Marzilli, *J. Chem. Soc., Chem. Commun.*, 1993, 1547–1548.
45 R. F. Pasternack, R. A. Brigandi, M. J. Abrams, A. P. Williams and E. J. Gibbs, *Inorg. Chem.*, 1990, **29**, 4483–4486.
46 C. Bustamante, S. Gurrieri, R. F. Pasternack, R. Purrello and E. Rizzarelli, *Biopolymers*, 1994, **34**, 1099–1104.
47 R. F. Pasternack, S. Gurrieri, R. Lauceri and R. Purrello, *Inorg. Chim. Acta*, 1996, **246**, 7–12.
48 T. M. Ou, Y. J. Lu, J. H. Tan, Z. S. Huang, K. Y. Wong and L. Q. Gu, *ChemMedChem*, 2008, **3**, 690–713.
49 Y. Mikami-Terao, M. Akiyama, Y. Yuza, T. Yanagisawa, O. Yamada and H. Yamada, *Cancer Lett.*, 2008, **261**, 226–234.
50 Y. Hori, M. C. Rogert, T. Tanaka, Y. Kikuchi, E. V. Bichenkova, A. N. Wilton, A. Gbaj and K. T. Douglas, *Biochim. Biophys. Acta*, 2005, **1730**, 47–55.
51 L. Lin and J. Hu, *J. Virol.*, 2008, **82**, 2305–2312.
52 A. Serganov and D. J. Patel, *Nat. Rev. Genet.*, 2007, **8**, 776–790.
53 D. L. Akins, H. R. Zhu and C. Guo, *J. Phys. Chem.*, 1996, **100**, 5420–5425.
54 E. D. Sternberg and D. Dolphin, *Tetrahedron*, 1998, **54**, 4151–4202.

